MODELLING OF HARMONICS PRODUCED BY COMPACT FLUORESCENT LAMPS IN THE FREQUENCY RANGE 2-150 KHZ

Caroline LEROI
Université catholique de Louvain
Belgium
caroline.leroi@uclouvain.be

Emmanuel DE JAEGER
Université catholique de Louvain
Belgium
emmanuel.dejaeger@uclouvain.be

ABSTRACT

This paper studies the disturbances produced by a device made of a rectifier with an active power factor correction. In particular, it focuses on compact fluorescent lamps. Active Power Factor Correction allows to reduce the low frequency harmonics (below 2 kHz) but it induces components at frequencies located in the frequency range 2-150 kHz. This paper presents the complete model of a compact fluorescent lamp and the design of its components. To reduce the simulation time, a simplified model made of a current source and the EMI filter is developed. A comparison of both models is performed and allows us to validate this simplified model.

INTRODUCTION

For a few years, electromagnetic interference (EMI) due to conducted disturbances in the frequency range 2-150 kHz has become a real issue in the context of LV distribution grid. The European committee for electrotechnical standardization (CENELEC) has already published three reports concerning this topic [1][2][3]. These disturbances are produced by devices using power electronics with a switching frequency located in this frequency range.

These disturbing devices can be mainly classified in two categories. There are first the self-commutated inverters as in solar panels or in wind turbines for instance. The other category concerns rectifiers with Active Power Factor Correction (APFC) as in Compact Fluorescent Lamps (CFL) or in some electric vehicle chargers.

To understand how these disturbances interact with each other and propagate through the LV distribution grid, it is important to model the sources. This paper will be focused on the modelling of the second category of disturbing devices, i.e. rectifier with APFC. Since lighting represents an important part of the total household electricity consumption, CFL will be considered but the drawn conclusions and the methodology can be extended to other devices including a rectifier with APFC.

The first section of this paper describes the different blocks that constitute a CFL. The design of these blocks is also considered in this section. To reduce the simulation time, a simplified model is developed in the second section. This simplified model is made of a current source in parallel with the EMI filter. The methodology used to simplify the model is general and can be extended to all devices including power electronics. In the third section, the results of the simplified model are compared with the ones obtained with the complete model simulated using Matlab Simulink® environment and more specifically the SimPowerSystems toolbox. Finally, the results of experimental measurements available on the database Panda [4] are presented and compared to the developed model.

COMPLETE MODEL

The complete circuit of a CFL can be decomposed in three main parts. The closest part to the grid is the EMI filter. It is used to filter harmonics higher than 150 kHz in order to stay under the limits defined in CISPR standards.

Then, a diode rectifier is used to convert AC to DC. The APFC following the diode rectifier is required to maintain the power factor as close to unity as possible. It has to be noticed that all CFL do not contain an APFC but only the circuit with APFC is discussed in this paper.

Finally, a half-bridge and a tank circuit are used to obtain a high-frequency current needed to feed properly the lamp.

Figure 1 illustrates the different blocks composing a CFL.

Figure 1 Complete model of a CFL

In the following, the combination of the half-bridge and the tank circuit is called the DC-AC converter. Its design is described hereafter as well as the design of the APFC.

DC-AC converter and lamp

The DC-AC converter and the lamp are modelled by the circuit represented in Figure 2.

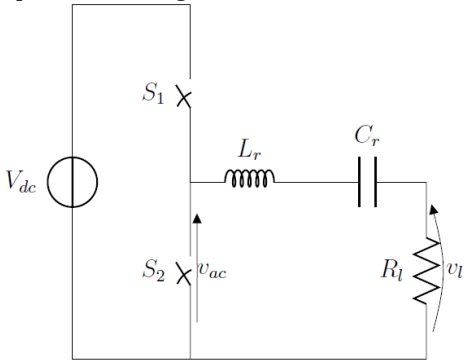

Figure 2 DC-AC converter and lamp

V_{dc} is the average value of the boost converter output voltage. v_{ac} is a rectangular periodical function. It is equal to V_{dc} during half of the period (when S_1 is closed) and equal to zero during the other half period (when S_2 is closed). The tank circuit ensures that the lamp voltage v_l keeps only the fundamental component of the voltage v_{ac}. This means that $v_l \approx \frac{2V_{dc}}{\pi}\sin(\omega_{hb}t)$.
The circuit elements values are then given by (1).

$$R_l = \frac{2V_{dc}^2}{\pi P_l}$$
$$L_r = \frac{QR_l}{\omega_{hb}} \quad (1)$$
$$C_r = \frac{1}{L_r\omega_{hb}^2}$$

With P_l the lamp power, ω_{hb} the switching frequency of the half-bridge and Q the quality factor of the tank circuit.

APFC

Several circuits exist to control the power factor but the most common one is the boost converter as shown in Figure 3.

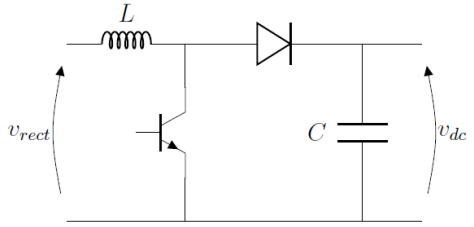

Figure 3 Active Power Factor Correction

v_{rect} is the rectified grid voltage. Neglecting the grid impedance, it is equal to $V_{peak}|\sin(\omega_g t)|$ with V_{peak} the peak grid voltage and ω_g the grid angular frequency.

The duty cycle of the boost θ is controlled in order to keep the output voltage v_{dc} constant and to provide a constant ratio between the instantaneous value of the inductance current and of the rectified voltage. This constant ratio is represented by an equivalent resistance R_{eq} equal to $\frac{V_{peak}^2}{2P_l}$.

Equation (2) represents the state equation of the current flowing through the inductance.

$$L\frac{di_l}{dt} = v_{rect} - v_{transistor} \quad (2)$$

On average, equation (2) becomes equation (3).

$$\frac{L}{R_{eq}}\frac{dv_{rect}}{dt} = v_{rect} - (1-\theta)V_{dc} \quad (3)$$

Replacing the rectified grid voltage by its equation, the waveform that the duty cycle must respect can be deduced.

$$\theta(t) = \begin{cases} 1 - r\sin(\omega_g t + \phi)\ from\ 0\ to\ \frac{T_g}{2} \\ 1 + r\sin(\omega_g t + \phi)\ from\ \frac{T_g}{2}\ to\ T_g \end{cases} \quad (4)$$

With

$$r = \frac{V_{peak}}{V_{dc}}\sqrt{1 + \left(\frac{L\omega_g}{R_{eq}}\right)^2}$$
$$\phi = \tan^{-1}\left(\frac{-L\omega_g}{R_{eq}}\right)$$

For the design of the capacitance, it is common to consider that its value is between 1 and 2µF per Watt.

Concerning the design of the inductance, it is chosen in order to limit the ripple current to a certain maximum value. Its minimum value to respect that limitation is given by (5).

$$L = \frac{V_{peak}\theta_{min}}{\Delta i_{max} f_{sw}} \quad (5)$$

With θ_{min} the minimum value of the duty cycle equal to $\frac{V_{dc}-V_{peak}}{V_{dc}}$, Δi_{max} the maximum allowed ripple and f_{sw} the switching frequency of the boost.

SIMPLIFIED MODEL

Complete simulation of circuits including switches takes time because it requires a very small time step. It is the main reason why a simplified model has to be developed. A simplified model is also useful to observe the influence of parameters more easily.

The simplified model proposed in this paper replaces the complete model by a current source in parallel with the EMI filter. This model is determined in three steps. Firstly, it is proved that the disturbances produced by the half-bridge are well attenuated and very small compared to the ones due to the APFC. Then, the APFC is replaced by a current source. Finally, the value of this current source on the AC side of the diode rectifier is developed.

Half-bridge simplification

Seen from the DC side, the half-bridge can be replaced by a current source. Assuming that the lamp current is only made of the fundamental, this current source is given by (6).

$$i_{hb}(t) = \frac{2V_{dc}}{\pi^2 R_l} + \frac{V_{dc}}{\pi R_l}sin(\omega_{hb}t) - \sum_{\substack{n=2 \\ n\ even}}^{\infty}\frac{4V_{dc}}{\pi^2 R_l(n^2-1)}\cos(n\omega_{hb}t) \quad (6)$$

It is therefore made of a DC component, a component at the switching frequency of the half-bridge and components at even multiples of this frequency.

Figure 4 shows the output circuit of the boost converter (Figure 3) with the half-bridge simplified by a current source.

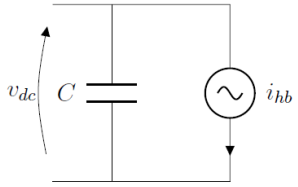

Figure 4 Half-bridge simplification

The transfer function between the half-bridge current and the dc voltage is given by (7).

$$\frac{\bar{V}_{dc}(j\omega)}{\bar{I}_{hb}(j\omega)} = -\frac{1}{j\omega C} \tag{7}$$

From this equation, it can be deduced that the components with a frequency higher than $\frac{1}{2\pi C}$ present in the half bridge current are attenuated. Considering that the power of a CFL is usually not less than 5W, it induces a minimum value for the capacitance of 5µF. Then, it means that components with a frequency higher than about 30 kHz are attenuated. Knowing that the switching frequency of the half-bridge typically lies between 45 kHz and 60 kHz, it can be concluded that the disturbances produced by the half bridge are attenuated quite well.

The circuit shown in Figure 4 is thus replaced by a constant DC voltage source V_{dc}.

APFC simplification

To be able to simplify the APFC, a development in Double Fourier series of its switching function is performed. It is based on the theory explained in [5]. The switching function is defined as equal to +1 when the duty cycle, governed by equation (4), is higher than the carrier and equal to 0 when it is lower. The carrier is a saw tooth signal with a frequency f_{sw}.

The double Fourier series of the switching function is developed in (8).

$$S(x,y) = \frac{1}{2}A_{00} + \sum_{n=1}^{\infty} A_{0n}\cos(ny) + B_{0n}\sin(ny) + \sum_{m=1}^{\infty}\sum_{n=-\infty}^{\infty} A_{mn}\cos(mx+ny) + B_{mn}\sin(mx+ny) \tag{8}$$

With

$$x = \omega_{sw}t$$
$$y = \omega_g t + \phi$$

$$A_{mn} + jB_{mn} = \frac{1}{2\pi^2}\left[\int_{\phi}^{\pi+\phi}\int_{0}^{2\pi(1-r\sin(y))} e^{j(mx+ny)}dxdy + \int_{\pi+\phi}^{2\pi+\phi}\int_{0}^{2\pi(1+r\sin(y))} e^{j(mx+ny)}dxdy\right] \tag{9}$$

Only the components with n even are different from zero.

The switching function is actually made of frequency components linked to the duty cycle which is its modulating wave and of frequency components around multiples of the switching frequency.

$$S(t) = \theta(t) + \sum_{m=1}^{\infty}\sum_{n=-\infty}^{\infty} A_{mn}\cos(m\omega_{sw}t + n\omega_g t + n\phi) + B_{mn}\sin(m\omega_{sw}t + n\omega_g t + n\phi) \tag{10}$$

Equation (11) is obtained by developing equation (9).

$$\begin{aligned} A_{mn} &= \frac{1}{m\pi^2}\int_{\phi}^{\pi+\phi}\sin(-mr2\pi\sin(y) + ny)\,dy \\ B_{mn} &= \frac{-1}{m\pi^2}\int_{\phi}^{\pi+\phi}\cos(-mr2\pi\sin(y) + ny)\,dy \\ B_{m0} &= \frac{1}{m\pi} - \frac{1}{m\pi^2}\int_{\phi}^{\pi+\phi}\cos(mr2\pi\sin(y))\,dy \end{aligned} \tag{11}$$

These integrals cannot be solved analytically but they can easily be solved numerically.

It can be observed that if the angle ϕ is neglected, the term B_{mn} can be rewritten using the definition of Bessel function of the first kind.

$$B_{mn} \approx \frac{-1}{m\pi}J_n(mr2\pi) \tag{12}$$

Once the switching function is developed, other variables can be obtained. Indeed, the transistor voltage can be expressed using the switching function as shown by (13).

$$v_{transistor} = \big(1 - S(t)\big)V_{dc} \tag{13}$$

Combining equations (2), (3), (10) and (13) the inductance current can be deduced.

$$i_l(t) = \frac{v_{rect}}{R_{eq}} + \sum_{m=1}^{\infty}\sum_{\substack{n=-\infty \\ n\ even}}^{\infty}\frac{\sqrt{A_{mn}^2 + B_{mn}^2}V_{dc}}{(m\omega_{sw} + n\omega_g)L}\sin\left(m\omega_{sw}t + n\omega_g t + n\phi + \tan^{-1}\left(\frac{A_{mn}}{B_{mn}}\right) - \frac{\pi}{2}\right) \tag{14}$$

The APFC circuit can therefore be replaced by a current source whose value is defined by equation (14). To simplify further computations, we note

$$I_{mn} = \frac{\sqrt{A_{mn}^2 + B_{mn}^2}V_{dc}}{(m\omega_{sw} + n\omega_g)L}$$
$$\psi_{mn} = n\phi + \tan^{-1}\left(\frac{A_{mn}}{B_{mn}}\right) - \frac{\pi}{2}$$

Diode rectifier simplification

The current taken from the grid is equal to the inductance current during half of the grid period and to minus this inductance current during the other half period.

Therefore, it can be demonstrated that the grid current contains only odd harmonics components and is given by equation (15).

$$i_g(t) = \sum_{\substack{h=1 \\ h\ odd}}^{\infty}\frac{4}{h\pi}\sin(h\omega_g t) \times i_l(t) \tag{15}$$

Replacing the inductance current by (14), equation (16) is deduced.

$$i_g(t) = \frac{v_g}{R_{eq}} + \sum_{m=1}^{\infty} \sum_{\substack{n=-\infty \\ n\ even}}^{\infty} \sum_{\substack{h=1 \\ h\ odd}}^{\infty} \frac{2I_{mn}}{h\pi} \times \begin{bmatrix} \cos(m\omega_{sw}t + (n-h)\omega_g t + \psi_{mn}) \\ -\cos(m\omega_{sw}t + (n+h)\omega_g t + \psi_{mn}) \end{bmatrix} \quad (16)$$

With v_g the grid voltage. Equation (16) can be rewritten to be able to extract the magnitude and the phase of each frequency component.

$$i_g(t) = \frac{v_g}{R_{eq}} + \sum_{m=1}^{\infty} \sum_{\substack{\alpha=-\infty \\ \alpha\ odd}}^{\infty} \sum_{\substack{h=1 \\ h\ odd}}^{\infty} \frac{2}{\pi} \times \left[\left[\frac{I_{m(\alpha+h)}}{h} \cos(\psi_{m(\alpha+h)}) - \frac{I_{m(\alpha-h)}}{h} \cos(\psi_{m(\alpha-h)}) \right] \times \cos(m\omega_{sw}t + \alpha\omega_g t) - \left[\frac{I_{m(\alpha+h)}}{h} \sin(\psi_{m(\alpha+h)}) - \frac{I_{m(\alpha-h)}}{h} \sin(\psi_{m(\alpha-h)}) \right] \times \sin(m\omega_{sw}t + \alpha\omega_g t) \right] \quad (17)$$

The simplified model is thus made of a current source defined by equation (17) in parallel with the EMI filter. The current source contains a fundamental component and components around multiples of the APFC switching frequency. Equation (17) allows us to study the disturbance frequency by frequency.

COMPLETE AND SIMPLIFIED MODELS COMPARISON WITH A NUMERICAL EXAMPLE

A numerical example is chosen in order to compare the grid current harmonics obtained with both models. The parameters values are:
$P_l = 30W$, $V_{dc} = 700V$, $Q = 20$, $f_{hb} = 50\ kHz$, $V_{g,RMS} = 230V$, $\Delta i = 0.15I_{max}$, $f_{sw} = 30kHz$, $f_g = 50Hz$, and $C = 2\mu F \times P_l$.

The EMI filter is not taken into account in this study as it remains the same in the simplified model.

The current on the grid side obtained with the complete model is illustrated in Figure 5 for the time domain and for the frequency domain.

It can be observed that the average current is a sinewave in phase with the voltage and that there are peaks in the spectrum around multiples of the boost switching frequency. With the EMI filter, these peaks would be lower especially for frequencies near 150 kHz.

With the chosen capacitance value, frequency components produced by the half bridge with a frequency higher than

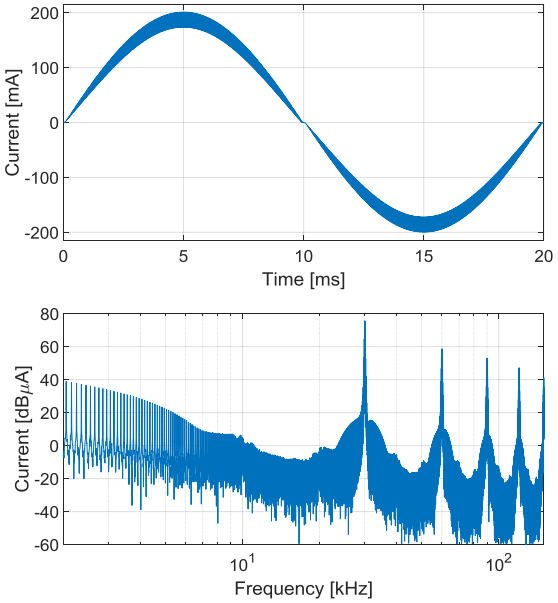

Figure 5 Grid current obtained with the complete model without taking into account the EMI filter. Time domain over 1 period (above) and frequency domain computed over 10 periods (below).

around 3 kHz are attenuated. At the frequency of the half-bridge, the attenuation factor is about 19, i.e. -25dB. It means that the voltage at the output of the boost converter can rightfully be approximated by its average value.

Figure 6 compares the magnitude of the grid current harmonics obtained with the complete model and with the simplified model. For the simplified model, the maximum value of h in equation (17) has been limited to 9.

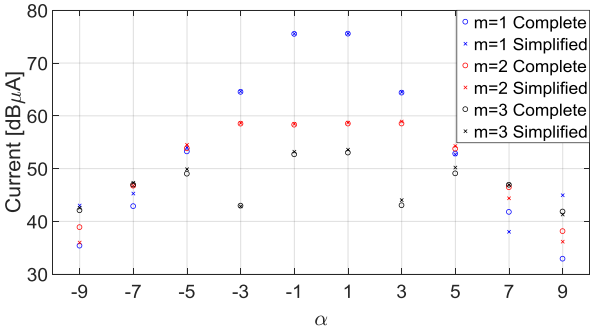

Figure 6 Comparison of the grid current harmonics magnitude obtained with the complete model and the simplified model

It can be concluded from Figure 6 that both models give very similar results. The ratio between both results is very close to one except for higher values of α for which the harmonics magnitude is negligible. The most representative frequency components are however well represented with the simplified model.

EXPERIMENTAL RESULTS

It has been demonstrated in the previous section that the results obtained with the simplified model are close to the

ones obtained with the complete model. To validate these models, they need to be compared with experimental measurements.

In the database Panda [4], the voltage and current to the terminals of several types of CFL have been tested. To be able to compute the frequency components up to 150 kHz, the sampling rate has to be higher than 0.3MS/s.

As a first step towards the validation of the developed models, the experimental results obtained for a same power CFL (30W) are used for a qualitative comparison. It is referred in Panda as the CDE-053 and has a power factor of 0.9721. Therefore, its circuit includes an APFC but the topology is not known. From the measurements results, the current in time domain and in frequency domain is plotted (see Figure 7).

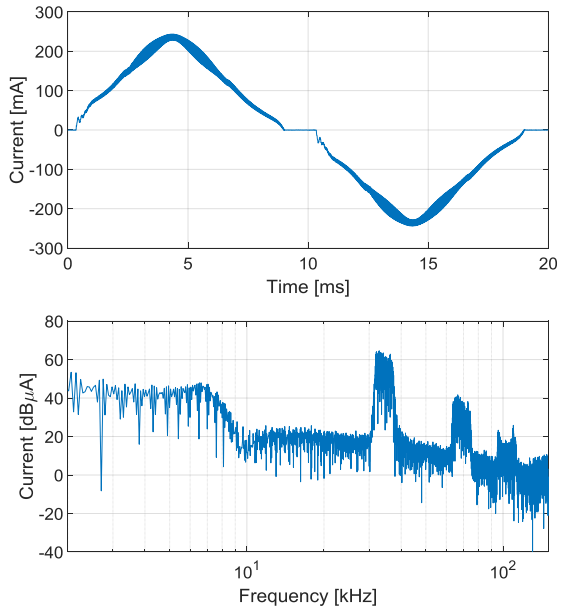

Figure 7 Measurements results of the current taken by the CDE-053 fed by a programmable voltage source. Time domain over one period (above) and frequency domain computed over 2 periods (below)

From the representation in the time domain, it can be noticed that the APFC does not work perfectly as in the developed complete model. Indeed, the power factor is different than one even if it is close. To be able to explain the differences, the circuit of the tested CFL should be known.

Concerning the representation in the frequency domain, it can be deduced that the switching frequency of the APFC is around 34 kHz. Peaks around multiples of this switching are also observed. These peaks magnitude is however lower than the one obtained in the developed complete model because of the EMI filter.

The EMI filter is a LC filter designed so that the cut-off frequency is given by equation (18).

$$f_c = \frac{f_d}{10^{\frac{Att_{req}}{40}}} \quad (18)$$

With f_d the first frequency multiple of the switching frequency above 150kHz and Att_{req} the required attenuation at this frequency in order to respect the standards.

CONCLUSION

The modelling of the disturbances produced by a rectifier with APFC has been dealt with. The case of the CFL has been taken as an example.

It has been concluded that the disturbances produced by the circuit upstream from the APFC can be neglected thanks to the capacitance placed at the output of the boost.

Eventually, all devices made of a rectifier with an APFC can be modelled by a current source defined by equation (17) in parallel with the EMI filter. This model can be used for further study. Indeed, it could be used to study the influence of some parameters on the magnitude of the disturbances or to study the propagation of these disturbances.

Furthermore, it has been demonstrated that the complete model and the simplified model give similar results. Experimental results have been presented but to be able to really validate the developed models, the EMI filter should be included and experiments should be carried out on several CFL with a high power factor as well as on other devices containing a rectifier with APFC.

In this paper, the harmonics have been computed by first developing in Double Fourier series the switching function. This methodology is general and can be extended to other devices including power electronics such as inverters for instance.

REFERENCES

[1] CENELEC, 2010, *SC205A - Main communicating systems - TF EMI - Study report on electromagnetic interference between electrical equipment / systems in the frequency range below 150kHz.*

[2] CENELEC, 2013, *SC205A - Main communicating systems - TF EMI - Study report on electromagnetic interference between electrical equipment / systems in the frequency range below 150kHz (2nd edition).*

[3] CENELEC, 2015, *SC205A - Main communicating systems - TF EMI - Study report on electromagnetic interference between electrical equipment / systems in the frequency range below 150kHz (3rd edition).*

[4] Technische Universität Dresden, *Panda – equiPment hArmonic DAtabase, https://www.panda.et.tu-dresden.de/*

[5] H.S. Black, 1953, *Modulation theory*, D. Van Nostrand Company, Princeton, United States of America.